Journal of Engineering Physics and Thermophysics, Vol. 68, No. 1, 1995

NUMERICAL SIMULATION OF THE AXISYMMETRIC LOW-VELOCITY FLOW AROUND A CYLINDER WITH COAXIAL DISKS

S. A. Isaev

UDC 532.517.4

The mechanism of reduction of the motion drag of a cylinder with coaxial disks is analyzed on the basis of a numerical solution of the Reynolds equations completed by a dissipative two-parameter model of turbulence.

1. The concept of controlled separation of a flow, promising in aerohydromechanics, has been developed consistently in some recent publications concerned with numerical solution and physical simulation of an axisymmetric incompressible viscous flow around a cylinder with a disk mounted in front of it. A study carried out in [1] to investigate the effect of physical viscosity on the structure of an artificially induced separated flow and the drag of a cylinder with a large aspect ratio has revealed that a thin disk mounted in front of the end face induces pronounced restructuring of the flow pattern and a substantial (severalfold) decrease of the profile drag. In this case, as soon as a front separation region (FSR) appears whose intensity rises with increase in the Reynolds number, the set of developed large-scale vortices near the lateral surface of a single cylinder disappears, and the flow around it becomes smooth and stable, which is inherent in the case of smooth streamline bodies. Numerical calculations have revealed rational configurations of a cylinder with a disk, which have minimum motion and profile drags. It is interesting that they differ somewhat because of a substantial effect of the FSR on the viscous friction of a long cylinder.

These conclusions were verified by the authors of [2], who analyzed a turbulent flow around a cylinder with a high aspect ratio with a protruding disk. For a cylinder with the aspect ratio $\lambda = 7$ (the ratio of the linear dimensions to the diameter) with the relative diameter of the disk $d_p = 0.75$ and the length of the protrusion $l_p = 0.375$, the drag coefficient C_x has a minimum value of 0.29 and the contributions of the friction and bottom drags are the highest, being 50% and 40%, respectively. Arrangements with the optimum C_x are comparable with streamline configurations such as a hemispherically blunted cylinder. The 20-fold decrease in the profile drag of this type of arrangement as compared with a single cylinder found earlier in Roshko–Koenig's experiments [3] have been confirmed numerically.

A thorough numerical investigation of the mechanism of reduction of the profile drag in the case of optimum arrangement ($d_p = 0.75$, $l_p = 0.375$) of a cylinder with a high aspect ratio with a front disk reported in [4] has revealed the decisive role of a large-scale vortex with extremely high intensity generated specially in the FSR. In that work emphasis is placed on an analysis of very fine effects connected with the effect of the turbulence Tu in the main flow on the structure of the flow in the FSR and on the motion drag. It is shown that in wind tunnel tests of bodies with this geometry there are very serious limitations in this important characteristic of wind tunnels since at Tu = 0.05 and 0.5% the data on C_x differ 1.5-fold, i.e., physical experiments can be conducted only in wind tunnels having a low turbulence level in the working section.

The authors of [5] who investigated an axisymmetric flow around step-shaped cylinders have shown that as the aspect ratio of the cylindrical section of bodies with an FSR decreases, the contribution of the friction drag dimishes sharply and the contribution of the bottom drag to the motion drag rises. For example, for a cylinder with the small aspect ratio $\lambda = 1.5$, the diameter of the protruding part $d = 0.73$, and the length of the protrusion $l_p = 0.3$, $C_x = C_{x\,\min} = 0.22$, 70% of which is due to C_{xd}.

Civil Aeronautical Academy, St. Petersburg, Russia. Translated from Inzhenerno-Fizicheskii Zhurnal, Vol. 68, No. 1, pp. 19-25, January-February, 1995. Original article submitted September 2, 1993.

 1062-0125/95/6801-0016$12.50

TABLE 1. Expressions for the Unknown Variable, Transfer Coefficients, and Source Term in Eq. (1)

φ	Γ_φ	S_φ
u	ν_{eff}	$1/y\partial/\partial x(\nu_{\text{eff}}y\partial u/\partial x)+\partial/\partial y(\nu_{\text{eff}}y\partial v/\partial x)-\partial/\partial x(p+2/3k)$
v	ν_{eff}	$1/y\partial/\partial x(\nu_{\text{eff}}y\partial u/\partial y)+\partial/\partial y(\nu_{\text{eff}}u\partial v/\partial y)-\partial/\partial y(p+2/3k)-$ $-2\nu_{\text{eff}}v/y^2$
k	$1/\text{Re}+\nu_t/\sigma_k$	$P-\varepsilon$
ε	$1/\text{Re}+\nu_t/\sigma_\varepsilon$	$\varepsilon/k(C_{\varepsilon_1}P-C_{\varepsilon_2}\varepsilon)$

Note. $\nu_{\text{eff}} = 1/\text{Re}+\nu_t$; $\nu_t = C_\mu f_c k^2/\varepsilon$; $f_c = 1/(1+C_c\text{Ri}_t)$; $P = \nu_t[2(\partial u/\partial x)^2+(\partial v/\partial y)^2+(\partial u/\partial y+\partial v/\partial x)^2]$.

TABLE 2. Set of Semiempirical Constants of the Modified Two-Parameter Model of Turbulence

C_μ	σ_k	σ_ε	C_{ε_1}	C_{ε_2}	C_c
0.09	1.0	1.3	1.45	1.92	0.1

Just like the problem of reducing the profile drag discussed, the problem of reducing the bottom drag can have a solution within the concept of controlled flow separation. As follows from Morel and Bohn's experimental study [6], a disk with a small diameter mounted at a certain distance in the wake behind a blunt body, in particular, a thin disk, causes a substantial decrease in the motion drag of the composite of the two disks. Therefore, use of a similar approach for reduction of C_{xd} of a cylinder, including that with a front disk, seems efficient.

Thus, the objectives of the present article are: (a) to continue numerical investigation of the longitudinal flow around cylinders with protruding disks close to optimum ones in profile drag; (b) to analyze in detail one of the methods for decreasing the bottom drag of cylinders within the concept of controlled flow separation in the case of a disk located in the near wake behind the cylinder; (c) to synthesize arrangements of cylinders with small aspect ratios with protruding disks that are optimum in profile and bottom drags; d) to compare streamline shapes and cylinders with disks in the front and tail parts.

2. The calculation of a steady-state axisymmetric viscous incompressible flow around a cylinder with protruding disks is carried out on the basis of a finite-volume solution of the Reynolds equations completed by a dissipative two-parameter turbulence model written in cylindrical coordinates (x, y). The system of equations written in a divergent form for the generalized variable φ ($\varphi = u, v, k, \varepsilon$) has the form

$$\frac{1}{y}\left\{\frac{\partial}{\partial x}\left[yu\varphi-\frac{\partial}{\partial x}\left(\Gamma_\varphi y\frac{\partial\varphi}{\partial x}\right)\right]+\frac{\partial}{\partial y}\left[yv\varphi-\frac{\partial}{\partial y}\left(\Gamma_\varphi y\frac{\partial\varphi}{\partial y}\right)\right]\right\} = S_\varphi. \quad (1)$$

The quantities entering Eq. (1) are summarized in Table 1. The semiempirical constants present in the equation of transfer of turbulence characteristics and in the expression for the turbulent viscosity ν_t are given in Table 2. The initial equations are expressed in dimensionless form. The velocity of the main flow and the diameter of the cylinder are chosen as normalizatiion scales.

It should be noted that the divergent form used for writting the equations and source terms is useful for constructing a difference scheme, for which the conservation equations are satisfied within the round-off errors. In the work the modified k-ε turbulence model, including the effect of the curvature of the streamlines on the turbulence characteristics within the Leschzinner–Rodi approach, was used.

The additional semiempirical constant C_c introduced in the relation of the turbulent viscosity ν_t versus the turbulent Richardson number Ri_t has been chosen as a result of special methodical studies in solving test problems on a circulation flow in a square cavity [7] and on a separated flow behind a back-facing step and problems on a flow around bodies of various configurations such as a single disk, a set of disks, and a cylinder with a disk located in front of it [8].

For the present boundary-value problem on a flow around a cylinder with disks, parameters of the main flow and turbulence characteristics are prescribed at the inlet boundary, suitable for the conditions of aeroballistic

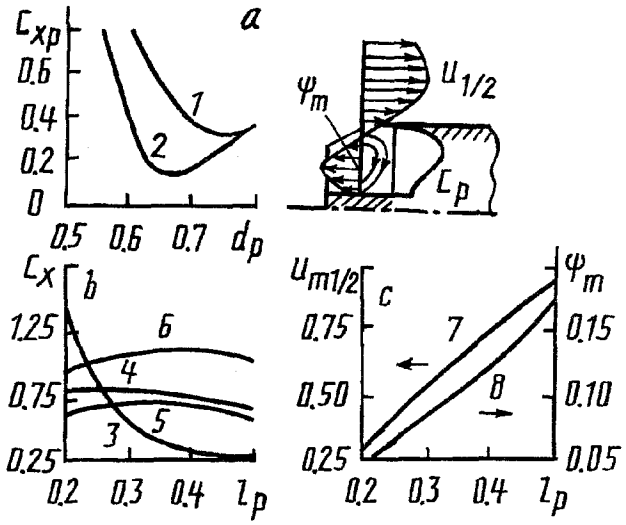

Fig. 1. Effect of the diameter d_p of the disk (a) and its protrusion l_p (at fixed d_p = 0.75) on the profile drag (a, b) and its components (b) for the arrangement of a semi-infinite cylinder with a disk and on the characteristics of a flow with an FSR (c): 1) l_p = 0.375; 2) 0.5; 3) $10C_{xp}$; 4) $C_{x\,dc}$; 4) $C_{x\,dc}$; 5) $-C_{x\,cl}$; 6) $-C_{pm}$; 7) $u_{m1/2}$; 8) ψ_m; a) $C_{xp}\cdot 10$.

experiments, mild boundary conditions are specified at the outlet boundaries, and conditions of symmetry are specified on the axis of symmetry. The well-tested apparatus of wall functions is used in the calculations.

The finite-volume algorithm is based on the concept of splitting over physical processes and is implemented as a unit-by-unit procedure with global iterations. It is constructed with the SIMPLEC method of pressure correction modified by Reitby and van Durmaal. Unlike the conventional variant, characteristic features of the algorithm developed in the present work are use of the Leonard counterflow quadratic scheme having low numerical diffusion for approximation of convective terms in the equations and solution of systems of algebraic equations with Buleev's incomplete matrix factorization in the SIP variant of Stone's method. It should be noted that stability of the computational procedure is also ensured by separation of Leonard's scheme into a counterflow scheme of the first order of approximation and a correcting term determined explicitly in the previous iterative step and written as an additional component in the source term. Thorough tests conducted in [7] have shown that the described specific features of the computational algorithm ensure reasonable accuracy and high efficiency of numerical simulation of complicated separated flows. It should be noted that convergence of the computation process was controlled by satisfaction of the condition of constancy (with specified accuracy of the order of magnitude of 10^{-3}) of the drag coefficient C_x and constancy of local turbulent characteristics at characteristic chosen points.

3. Calculation methods developed on the basis of the suggested algorithm have been used for simulation of an axisymmetric high-velocity flow around cylinders with protruding thin disks in the front and tail sections. The computations have been carried out on a staggered grid, containing 81 × 40 nodes with decreased spacing in the neighborhood of the body and at its sharp edges. The minimum step of the grid is 0.2. The thickness of the disks is neglected in the computations. The Reynolds number of the main flow is assumed to be $2\cdot 10^5$. In the numerical experiments the dimensions of the computation region are chosen from the condition of a very slight effect of them on the integral characteristics of the flow around the objects considered.

Analysis of the curves of the profile drag of a long cylinder with a protruding disk versus the diameter of the disk and the gap between the disk and the face of the cylinder shown in Fig. 1 inducates that there are arrangements of FSR bodies that are optimum in C_{xp}. It is interesting to note that C_{xp} are very low for a composite body whose components are classic blunt bodies such as a disk and a cylinder. As can be seen from Fig. 1a, for an arrangement with d_p = 0.63 and l_p = 0.5, it is possible to obtain C_{xp} = 0.016, i.e., the profile drag of such bodies can be decreased by two orders of magnitude as compared with a flat face. The mechanism of reduction of the profile drag is explained by analysis of the curves $C_{xp}(l_p)$ shown in Fig. 1b. In a wide range of the gap l_p, the

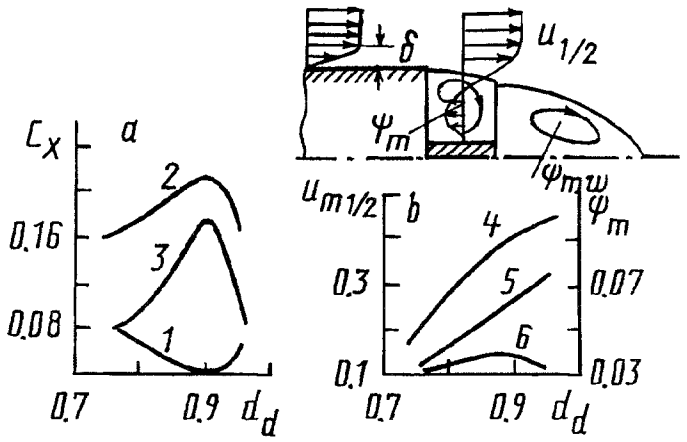

Fig. 2. Effect of the diameter d_d of the disk on the bottom drag and its components (a) for the arrangement of a semiinfinite cylinder with a disk and on the characteristics of the flow in the cavity between the disk and the cylinder and in the near wake (b): 1) C_{xd}; 2) $C_{x\,\mathrm{cl}}$; 3) $-C_{x\,\mathrm{dc}}$; 4) $C_{m1/2}$; 5) ψ_m; 6) ψ_{mw}.

cylindrical part is affected by a high thrust force $C_{x\,\mathrm{cl}}$ that compensates for the motion drag $C_{x\,\mathrm{dc}}$ of the protruding disk almost completely. As follows from Fig. 1b, it is induced by substantial rarefaction on the face of the cylinder (the pressure coefficient C_{pm} that is maximum in absolute value exceeds the rarefaction on the rear surface of the disk in a uniform flow more than 2.5-fold). An increase in the gap l_p stimulates an increase in the intensity of the circulating flow, determined by maximum velocities $u_{m1/2}$ in the middle cross section of the large-scale vortex and the stream function ψ_m in the FSR (Fig. 1c). It is important to note that $u_{m1/2}$ is comparable with the velocity of the main flow at l_p of the order of magnitude of unity.

Numerical simulation of the flow around a semi-infinite cylinder with a disk mounted in the tail section was conducted under the condition that a velocity profile varying within the thickness of the boundary layer δ = 0.15 as 1/7 is specified in the main flow at a certain distance from the edge of the cylinder. The effect of the diameter of the disk d_d at the fixed gap l_p = 0.375 (see Fig. 2a) indicates that deliberate induction of a large-scale vortex in the cavity between the disk and the face of the cylinder decreases substantially the bottom drag of the arrangement. When d_d = 0.9 is chosen, the bottom drag coefficient is 2.5 times lower than the C_{xd} of a single cylinder. Just like the effect of reduction of the profile drag, the effect of reduction of the bottom drag is caused by the thrust force induced under certain conditions and exerted on a thin disk located in the near wake. For arrangements of a cylinder with a disk that are rational in bottom drag, the bottom drag of the cylinder $C_{x\,\mathrm{cb}}$ is compensated substantially by the thrust force $C_{x\,\mathrm{dc}}$ exerted on the disk. As one can see from Fig. 2b, in this case the deliberately generated vortex is characterized by high intensity, which predetermines higher rarefaction on the disk from the side of the cavity as compared with the rarefaction in the near wake. It should be noted that an increase in the diameter of the disk results in intensification of the flow both in the large-scale vortex and in the wake. When the arrangement that is optimum in C_{xd} is chosen, the maximum velocity of the reverse flow is about 40% of the velocity of the main flow and the maximum stream function ψ_m is more than twice this quantity ψ_{mw} in the near wake behind a single cylinder but is half of ψ_m in the FSR for the arrangement of a cylinder with a front disk that is optimum in C_{xp}.

Thus, it can be concluded that deliberate generation of a separation region in the front and tail sections of a cylinder with a high aspect ratio decreases substantially the motion drag of the cylinder. The disk–cylinder–disk arrangement with the dimensions d_p = 0.75, l_p = 0.375, d_d = 0.9, l_d = 0.375 can be recommended as one that is optimum in C_x. In what follows this arrangement is referred to as basic.

As is known, the bottom drag of bodies of any geometry depends substantially on their aspect ratio and for a thin disk, which is a body of the lowest aspect ratio (~0.40), C_{xd} is four times as large as C_{xd} for a single cylinder with a large aspect ratio (~0.10). Therefore, the trend in the bottom drag of the basic arrangement consisting of a cylinder with disks to increase with a decrease in the aspect ratio λ of the cylindrical section shown

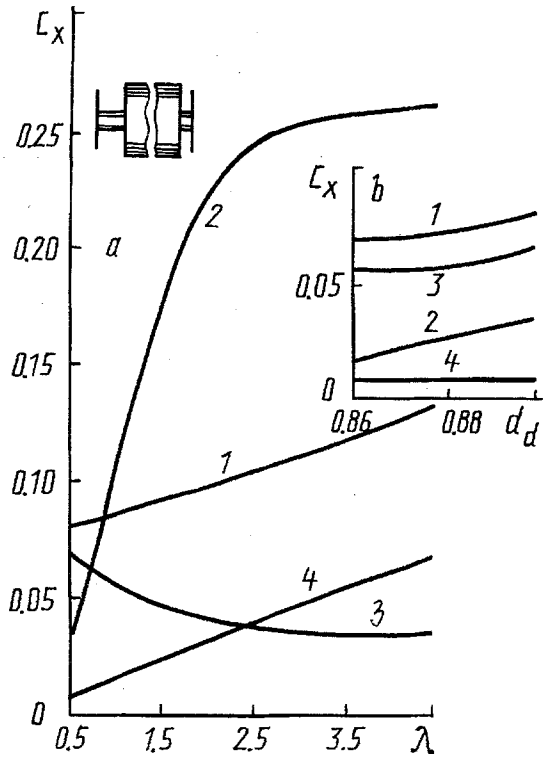

Fig. 3. Effect of the aspect ratio (a) and the diameter d_d of the rear disk (b) on the motion drag and its components for the basic disk–cylinder–disk arrangement (d_p = 0.75; l_p = 0.375; d_d = 0.9; l_d = 0.375) with the other parameters of the body of small aspect ratio λ = 0.5 being fixed: 1) C_x; 2) $10C_{xp}$; 3) C_{xj}; 4) C_{xd}.

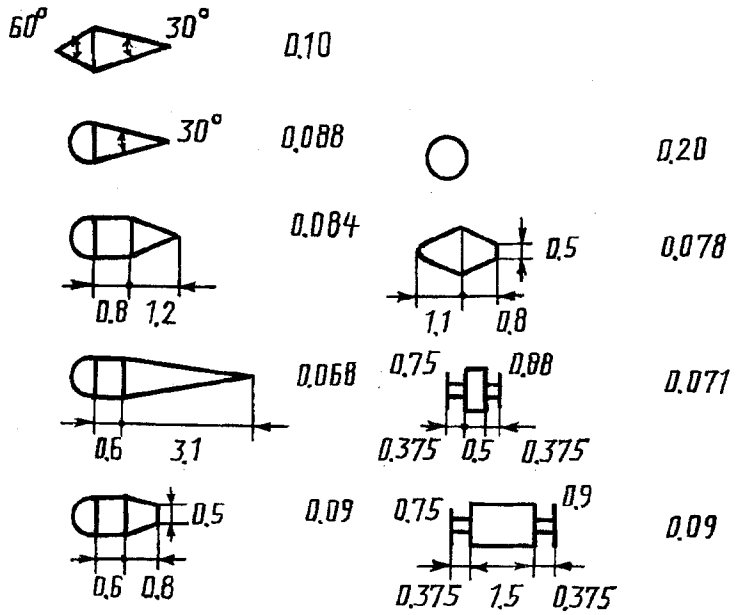

Fig. 4. Comparison of bodies of conventional shapes with cylinders with disks in a low-velocity flow ($Re = 2 \cdot 10^5$) in their motion drag.

in Fig. 3 seems quite reasonable. In particular, with λ = 0.5, C_{xd} is about 1.7 times higher than it is at $\lambda = \infty$. However, the very sharp decrease in the profile drag of the arrangements consisting of the considered bodies with a very low aspect ratio is somewhat unexpected. For short bodies (λ = 0.5) C_{xp} = 0.004, i.e., in profile drag these bodies are equivalent to the configuration of a hemispherical nose. It is indubitable that the extremely low profile

resistance of the bodies can be explained by the effect of a large-scale vortex generated in the bottom part on the flow in the FSR. It is interesting that bodies of the basic geometry are not optimum in bottom drag since the flow pattern for short bodies is different from the flow pattern for long bodies. A decrease in the gap d_d between the rear disk and the cylinder resulted in a slight decrease in the bottom drag of the arrangement. For example, at $d_d = 0.86-0.88$, C_{xd} is about 15% lower than C_{xd} for the basic arrangement at $d_d = 0.9$. It should be emphasized that in this case a reduction in the bottom drag is accompanied by a decrease in the profile drag. In particular, at $d_d = 0.86$, $C_{xp} \simeq 0.002$, i.e., it is half as large as for the basic configuration. It is interesting that the friction drag of a body of the basic geometry depends linearly on the aspect ratio of the cylindrical section λ, and any changes in the dimensions of the rear disk have almost no effect on the friction drag (for example, $C_{xf} \simeq 0.01$ for $\lambda = 0.5$). In general, the motion drag of the disk–cylinder–disk arrangement is much lower than the motion drag for bodies with an FSR. In particular, the motion drag of a cylinder (aspect ratio $\lambda = 1.5$) with a step-shaped nose with a geometry that is optimum in C_{xp} ($C_x = 0.22$ [4]) can be more than halved for a body with the basic configuration ($C_x = 0.09$).

In Fig. 4 various streamline bodies with a small aspect ratio, whose characteristics are taken from the monograph [9], are compared in the drag coefficient with the bodies of nonconventional shape considered. It is evident that the latter bodies have indubitable structural merits, and in C_x, they are not inferior and occasionally even superior to streamline bodies of simple geometry. This makes nonconventional bodies promising as rational forms of engineering devices for various purposes, in particular containers and other freight with external suspension transported by helicopters, deep-sea apparatus, buoys, floating drilling platforms, vans, refrigerators, and tanks.

NOTATION

x, y, axial and radial coordinates; d, l, relative diameter of the disk and length of its protrusion in front of the end face of the cylinder; u, v, axial and radial velocity components; k, turbulence energy; ε, dissipation rate of turbulence energy; Re, Reynolds number; Ri_t, turbulence Richardson number; Tu, turbulence of the main flow; ν_i, turbulent viscosity; λ, aspect ratio of the cylindrical part of the body; C_p, coefficient of excess static pressure relative to the pressure in the main flow; C_x, C_{xp}, C_{xd}, C_{xj}, coefficients of motion, profile, bottom, and friction drags; ψ, stream function; φ, unknown generalized variable; Γ_φ, diffusion transfer coefficient; S_φ, source term; P, term of generation of turbulence energy; C_μ, σ_k, σ_ε, $C_{\varepsilon 1}$, $C_{\varepsilon 2}$, C_c, semiempirical constants; f_c, correction function including the effect of curvature of streamlines on the turbulence characteristics. Subscripts and superscripts: min, m, minimum and maximum values; 1/2, parameters determined in the middle cross section of the cavity between the disk and the cylinder; cl, integral characteristic for a cylinder; dc, integral characteristic for a disk; p, parameter characterizing the FSR; d, parameter characterizing the deliberately generated separation region in the bottom part; w, parameter in the near wake.

REFERENCES

1. V. R. Bobyshev, S. A. Isaev, and O. L. Lemko, Inzh.-Fiz. Zh., **51**, No. 2, 224-232 (1986).
2. V. R. Bobyshev and S. A. Isaev, in: Turbulent-Transfer Processes [in Russian], Minsk (1988), pp. 39-48.
3. V. K. Bobyshev and S. A. Isaev, Inzh.-Fiz. Zh., **58**, No. 4, 556-572 (1990).
4. S. A. Isaev, V. M. Suprun, and O. A. Shul'zhenko, Inzh.-Fiz. Zh., **60**, No. 3, 433-439 (1991).
5. K. Koenig and A. Roshko, J. Fluid Mech., **156**, 167-204 (1985).
6. T. Morel and M. Bohn, Teor. Osnovy Inzhener. Raschyotov, **102**, No. 1, 225-234 (1980).
7. I. A. Belov, S. A. Isaev, and V. A. Korobkov, Problems and Methods of Calculation of Incompressible Separation Flows [in Russian], Leningrad (1989).
8. S. A. Isaev, Vestsi Akad. Navuk BSSR, Ser. Fiz.-Énerg. Navuk. No. 4, 57-62 (1989).
9. V. I. Egorov, Underwater Towing Vehicles [in Russian], Leningrad (1981).